JOURNAL OF OPTOELECTRONICS AND ADVANCED MATERIALS, Vol. 11, No. 5, May 2009, p. 590 - 596

Background gas driven photoemission from laser ablated Li^+ doped $Gd_2O_3:Eu^{3+}$ thin films

GEO RAJAN, K. G. GOPCHANDRAN*
Department of Optoelectronics, University of Kerala Kariavattom, Thiruvananthapuram-695 581, India

High quality $Gd_{1.82}Eu_{0.10}Li_{0.08}O_3$ thin films have been deposited on quartz substrate under oxygen, nitrogen and argon reactive atmospheres using pulsed laser deposition technique. The influence of various reactive atmospheres on the structural, morphological and optical properties were investigated systematically using X-ray diffraction (XRD), atomic force microscopy (AFM) and photoluminescence spectroscopy (PL). The crystalline phase, surface morphology and surface roughness were found to be very sensitive to the ambient gas, which was used during deposition. The highest emission intensity was observed for the films grown under oxygen reactive atmosphere, whose brightness was 1.52 and 5.97 times higher than that of the films grown under nitrogen and argon ambient atmospheres. The films prepared under nitrogen ambient atmosphere, the intensity ratio of the 612 nm peak to that of 624 nm peak was found to be higher than that of films deposited under oxygen and argon atmospheres.

(Received May 10, 2009; accepted May 25, 2009)

Keywords: Thin film, Gd_2O_3:Eu, Li-doped, Laser ablation, Photoemission

1. Introduction

Luminescent materials can be found in a broad range of every day applications such as cathode ray tubes (CRTs) [1] projection television screens, electroluminescent devices (ELEDs), plasma display panels (PPDs) [2] and field emission displays [3]. Displays with nano-size phosphors have a higher contrast and resolution, superior thermal conductivity, high packing density and better adhesion [4]. Phosphor nanoparticles have been extensively studied in both fundamental and technological research [5, 6]. It is anticipated that oxide phosphors have the potential for replacing conventional displays. Lanthanide activated rare-earth oxides[7,8] remain as promising materials for next generation display technology because of several essential superior properties such as luminescent characteristics, stability in vacuum and corrosion free gas emission under electron bombardment compared with traditional cathode ray tube red phosphors used in current field emission displays[9,10]. Among the oxide based phosphors, $Gd_2O_3:Eu^{3+}$ thin films were proposed as one of the most promising oxide based red phosphor systems. Due to the $^5D_0$-$^7F_2$ transition within europium, $Gd_2O_3:Eu^{3+}$ shows red luminescence properties and emits red light at 612 nm wavelength [11, 12]. Therefore, oxide-based phosphors are likely to emerge as the choice for FED red phosphors. In thin film phosphors brightness may be associated with several factors such as (i) the interaction between the generated beam material and substrate, (ii) the film processing conditions, and (iii) the composition of the film materials. Among these factors the film processing conditions and the composition could be one of the lead breakthroughs for increased brightness of $Gd_2O_3:Eu^{3+}$ thin films. It is well known that even in very small quantities, the Li^+ co-activators frequently play an important role in the enhancement of the luminescent efficiency of phosphors [7]. Yi *et al.* reported that the photoluminescent (PL) brightness of Li^+ doped $Gd_2O_3:Eu^{3+}$ films are 2.1 to 2.3 times greater than that of undoped $Gd_2O_3:Eu^{3+}$ films [13, 14, 15]. In previous studies nano-sized $Gd_2O_3:Eu^{3+}$ phosphor materials have been prepared using solid state reactions [16], hydrothermal method[17], co-precipitation methods[18], sol-gel methods[19,20], spray pyrolysis [21], chemical vapour deposition[22] and pulsed laser deposition technique(PLD)[12, 14, 15]. In PLD, one can control size distribution and shape of nanocrystals by varying the parameters like target to substrate distance, laser fluence, back ground gas pressure, substrate temperature etc; and thus it emerges as an effective tool for the growth of quantum structures with high chemical purity and controlled stoichiometry [23]. During the deposition of oxide thin films by PLD, the reactive atmosphere is a critical deposition parameter. The presence of the background gas during irradiation fundamentally changes the mechanism of formation of nanoparticles [24, 25]. In this article, $Gd_{1.82}Eu_{0.10}Li_{0.08}O_3$ thin films were prepared by PLD in different reactive atmospheres and the effect on the micro-structural, morphological and luminescence properties were discussed.

2. Experimental

Gd_{2-x-y} $Eu_xLi_yO_3$(x=0.10, y =0.08) powder samples (were of 99.99 % purity, Sigma-Aldrich) were prepared from stoichiometric amounts of Gd_2O_3, Eu_2O_3 and Li_2O_3. For a ceramic target, the powder mixture was pelletized into a disc and sintered at 1623 K for 10 h. The films were grown on quartz substrate by pulsed laser deposition

(PLD) technique, using a Q-switched Nd:YAG laser, (Quanta - ray INDI-Series, Spectra-Physics) with 12 J cm^{-2} laser fluence at 532 nm, pulse width 8 ns, and repetition frequency 10 Hz. Target substrate - distance was 6 cm and the deposition time was 30 minutes. The films were deposited in oxygen, nitrogen and argon reactive atmospheres under an ambient pressure of about 50 mTorr and an optimum substrate temperature of about 873 K. The crystallinity of thin film phosphors were examined using grazing incidence X-ray diffraction (GIXRD) (Siemens D5000 diffractometer) measurements using Cu K□ radiation with a wavelength of 0.15406 nm. Surface morphology of the deposited films at nanometric scale was investigated by AFM (Digital Instruments Nanoscope E) measurements in contact mode. Particle size and root mean square (rms) surface roughness of the deposited films were determined on a scan area of 500 x 500 nm. Photoluminescence spectra of the samples were recorded by Horiba Jobin Yvon Flourolog (III) modular spectroflourophotometer equipped with 450 W Xenon lamp and Hamatsu R928-28 photomultiplier.

3. Results and discussion

3.1 X-Ray diffraction studies

Fig. 1 shows the GIXRD patterns of $Gd_{1.82}Eu_{0.10}Li_{0.08}O_3$ thin films deposited on quartz substrates under different reactive atmospheres. All the diffraction patterns were indexed according to the ASTM data card No: 88-2165 for cubic and No: 43-1015 for monoclinic Gd_2O_3. In the case of film grown under oxygen reactive atmosphere (Fig.1 (a)) the film possess a mixed structure of both cubic(C) and monoclinic (M) Gd_2O_3. It can be seen that the (222) peak of cubic Gd_2O_3 as well as (402) peak of monoclinic Gd_2O_3 were almost equally predominant, which strongly indicates the formation of random orientation. No trace of cubic structure was detected in films deposited under nitrogen and argon atmospheres. In the case of films grown under nitrogen atmosphere, corresponding to monoclinic Gd_2O_3, the preferential orientation is along (402) lattice plane. The concentration of oxygen vacancy in the film depends on the oxygen partial pressure during the film deposition and which intern results in preferential growth in other directions [26]. John *et al.* reported that the change in the film orientation is associated with an increased number of out growths which act as nucleation centers for grains of other orientations [27]. A peak (111) corresponding to monoclinic Gd_2O_3 was appeared in the films grown under nitrogen and argon ambient atmospheres. Under argon atmosphere the (402) peak become more prominent as compared with the films in nitrogen atmosphere. From this result it can be concluded that the reactive atmosphere has a strong influence on the structure of $Gd_{1.82}Eu_{0.10}Li_{0.08}O_3$ films. The average size of nano-particles in the films were estimated using Debye-Sherrer relation [28] and the average size of nano-particles were found to be 35.7, 23.6 and 24.8 nm for the films deposited under oxygen, nitrogen and argon reactive atmospheres respectively.

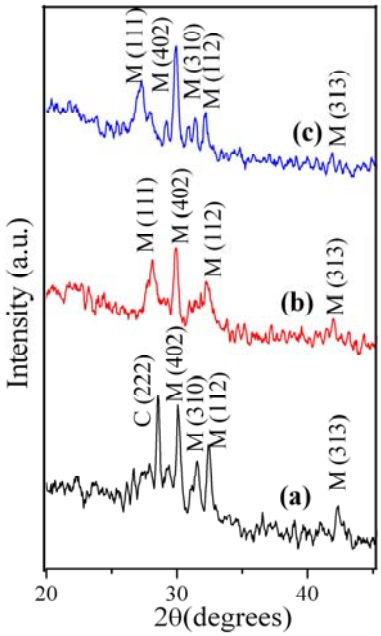

Fig. 1. GIXRD patterns of $Gd_{1.82}Eu_{0.10}Li_{0.08}O_3$ thin films deposited on quartz substrates under (a) oxygen (b) nitrogen and (c) argon reactive atmospheres at 50 mTorr.

3.2 AFM Analysis

The AFM images of $Gd_{1.82}Eu_{0.10}Li_{0.08}O_3$ thin films deposited on quartz substrates under different reactive atmospheres is shown in Fig. 2. It can be seen from the AFM images that the growth of the film is normal to the surface for the films deposited in argon and nitrogen atmospheres, even though size of the particles are different. A film deposited in oxygen atmosphere possesses a morphology consisting of particles, spherical granular in shape with a growth pattern agreeing with the observed random orientation in the XRD pattern (Fig.1 (a)). The high value of RMS roughness of these films deposited in oxygen atmosphere may be due to the distribution of molecules and clusters are not uniform along the plume axis. The variation in nature and size of particles in $Gd_{1.82}Eu_{0.10}Li_{0.08}O_3$ thin films prepared under different atmospheres may be accounted to the fact that vapor species undergo enough collisions so that nucleation of these vapor species to form particles can occur before their arrival at the substrate and the life time of the particles in the respective vapor controls its size [29, 30]. The longer the life time, as is the case with increased

molecular weight of the back ground gas, the larger the size of the particles [29]. But in argon reactive atmosphere, its first ionization energy is high and hence the ambient gas pressure can affect the impinging kinetic energy of the ions on the substrate surface, and is resulting in a significant fraction of the atoms deposited on the substrate can sputter from that substrate itself due to the bombardment by high-energy particles in the incoming flux of atoms and ions.

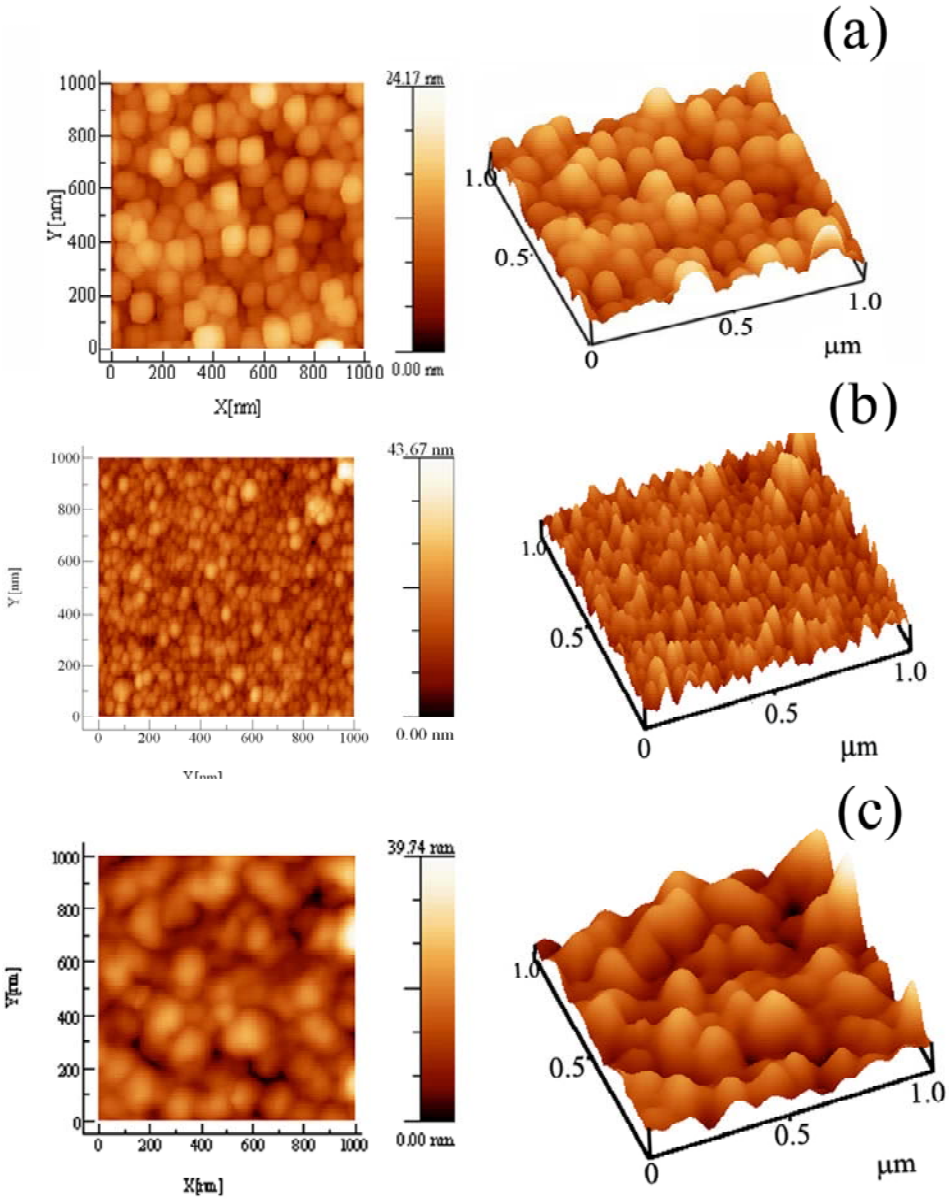

Fig. 2. AFM images (2D & 3D) of $Gd_{1.82}Eu_{0.10}Li_{0.08}O_3$ thin films deposited on quartz substrates under (a) oxygen (b) nitrogen and (c) argon reactive atmospheres at 50 mTorr.

3.3 Luminescent Properties

Fig. 3 shows the photoluminescence spectra of $Gd_{1.82}Eu_{0.10}Li_{0.08}O_3$ thin films deposited on quartz substrates under different reactive atmospheres and the inset shows the corresponding excitation spectra. The excitation spectra were obtained by monitoring the emission of Eu^{3+} due to the transition $^5D_0$-$^7F_2$ at 612 nm. It can be seen from the inset of Fig.3, that the excitation spectrum consists of a broad intense band with a maximum at 265 nm and a shoulder around 274 nm, whose intensity is maximum for the films deposited under oxygen reactive atmosphere. The increased excitation intensity may be due to the presence of considerable amount of cubic phase of Gd_2O_3 host lattice. The broad absorption peak at 265 nm is due to the charge transfer

from the O 2p state to the charge – transfer state (CTS) of the Eu^{3+} ion [31]. The charge transfer transition takes place because of the Eu^{3+} ion ($4f^6$ configuration) tends to capture an electron from the from the O 2p state in order to achieve a more stable half filled shell state ($4f^7$ configuration[32].

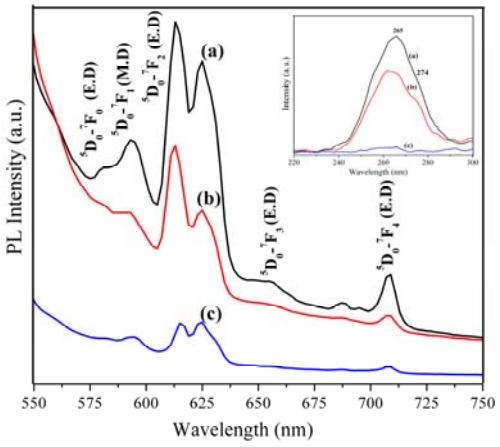

Fig.3 Photoluminescence spectra of $Gd_{1.82}Eu_{0.10}Li_{0.08}O_3$ thin films deposited on quartz substrates under (a) oxygen (b) nitrogen and (c) argon reactive atmospheres at 50 mTorr. The inset shows the corresponding excitation spectrum.

Excitation into the Gd_2O_3 host band at 265 nm yields the emission corresponding to f-f transitions of Eu^{3+} ion which were dominated by the hypersensitive $^5D_0$-$^7F_2$ at 612 nm. The characteristic PL emission involves transitions from the excited $^5D_0$ level to the crystal field split ^7F_J manifolds of the $^4F_6$ electronic configuration. In europium, the $^5D_0$-^7F_J is a very sensitive probe of the crystal field around the Eu^{3+} site. In Eu^{3+}, $^5D_0$-$^7F_{1,3}$ emission is an allowed magnetic dipole transition and $^5D_0$-$^7F_{2,4}$ is a forbidden electric dipole transition(parity selection rule)[33]. This selection rule can be relaxed when Eu^{3+} is placed in a host lattice like Gd_2O_3 which lacks in inversion symmetry. It is well known that in a cubic Gd_2O_3 lattice two distinct sites are available for rare earth doping, i.e.; sites with C_2 or C_{3i} (S_6) point group symmetry [11]. The rare earth ion occupying C_{3i} site possesses a center of inversion symmetry making the $^5D_0$-$^7F_{2,4}$ optical transitions strictly forbidden. Therefore the dominant $^5D_0$-$^7F_{2,4}$ rare earth emission lines originate from forced electric dipole transitions of the Eu^{3+} ion occupying C_2 sites with a lack of inversion symmetry and from allowed magnetic dipole transitions. More specifically the forced electric dipole transitions for Eu^{3+} ($^5D_0$-$^7F_{2,4}$) are hyper sensitive to the host crystallographic symmetry [33]. The monoclinic Gd_2O_3 provides three different C_s crystallographic sites for the Eu^{3+} ion [12]. These three sites give rise to a majority of the $^5D_0$ and $^7F_2$ stark levels which produce numerous peaks in the range 600 to 640 nm, even though our measurement was not sufficient to resolve them. Hence in Eu^{3+} ion in different Gd_2O_3 crystal structures show different emission lines.

The optical signatures of $Gd_{1.82}Eu_{0.10}Li_{0.08}O_3$ films deposited under different reactive atmospheres are shown in Fig. 3 and the films deposited under oxygen and nitrogen reactive atmospheres are anticipated to be identical but differ in their intensity. The enhanced PL intensity of the films prepared under oxygen reactive atmosphere may be due to the presence of considerable amount of cubic Gd_2O_3. It agrees well with the result that the monoclinic system shows a considerably lower luminescence than cubic system at 612 nm [11]. However the intensities of the 612 nm peak with respect to 624 nm peak (I_{612}/I_{624}) is found to be different in these films and the variation is depicted in Fig. 4. The intensity ratio is maximum for the film deposited in nitrogen reactive atmosphere. The increased intensity ratio of these films may be due to the occupation of Eu^{3+} ions in a new surface site, brought on by the increased surface strain of the film. The difference in intensity ratio of the films deposited in various reactive atmospheres may be due to difference in number of Eu^{3+} ions occupying in the film surface.

The $^5D_0$-$^7F_1$ transition of Eu^{3+} is a magnetic dipole allowed and its intensity shows very little variation with local environments surrounding Eu^{3+}, while the $^5D_0$-$^7F_2$ transition is electric dipole allowed and its intensity is sensitive to the local structure around Eu^{3+}[34]; therefore the intensity ratio of the electric dipole to the magnetic dipole transition has been widely used for investigating the chemical bonding of anions coordinating the rare earth ions. Fig.4 shows the variation of PL intensity ratio between electric-dipole to magnetic-dipole transition in the films prepared under different reactive atmospheres. It can be seen that the proportion of emission intensity due to the contribution of $^5D_0$-$^7F_2$ transition decreases when the reactive atmosphere changes from oxygen to nitrogen and to argon is an indicative of the increase in symmetry of the local environments surrounding the Eu^{3+} ion [35].

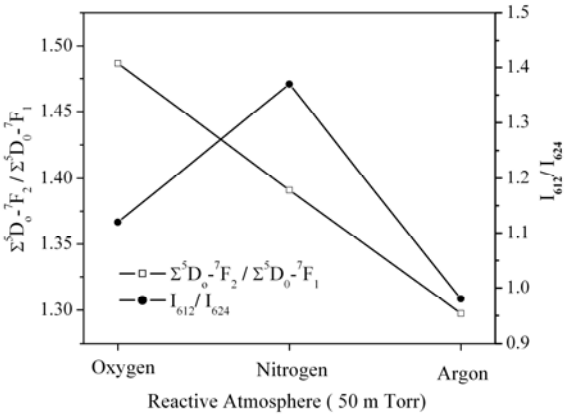

Fig. 4 The variation in PL intensity ratio of $^5D_0$-$^7F_2$ transition to $^5D_0$-$^7F_1$ transition and the intensity ratio of 612 nm peak to 624 nm peak of the films deposited under different reactive atmospheres.

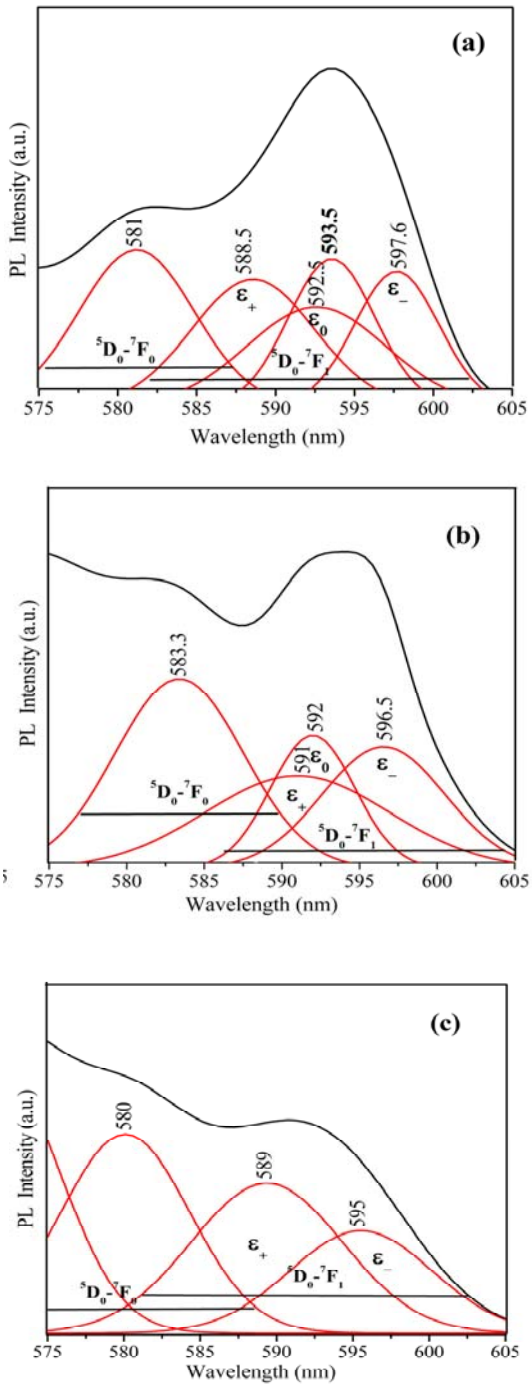

Fig. 5. Resolved emission spectra of the three crystal field splitting lines of the $^5D_0$-$^7F_1$ and $^5D_0$-$^7F_0$ transition of $Gd_{1.82}Eu_{0.10}Li_{0.08}O_3$ films deposited under (a) oxygen, (b) nitrogen and (c) argon atmospheres.

Fig. 5 shows the resolved emission spectra of the crystal field splitting lines of $^5D_0$-$^7F_1$ and $^5D_0$-$^7F_0$ transition of the films deposited under various reactive atmospheres. The $^5D_0$-$^7F_1$ transition should have three stark splitting peaks.

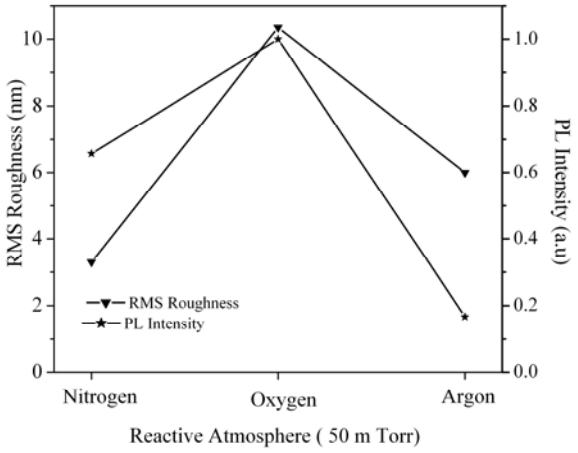

Fig. 6. Plots of PL intensity and surface roughness of $Gd_{1.82}Eu_{0.10}Li_{0.08}O_3$ films prepared under different reactive atmospheres.

As shown in Fig. 5, the lines of $^5D_0$-$^7F_1$ transition can be resolved into three Gaussian components ε_-, ε_0 and ε_+ [36]. From the detailed analysis of the stark splitting peaks originated from the $^5D_0$-$^7F_1$ transition, it is obvious that the peak positions of the Gaussian components are very much sensitive to the nature of the ambient atmosphere during deposition. The ε_0 component is absent in the film deposited under argon atmosphere may be due to the lower PL intensity of the sample.

Fig. 6 exhibits the correlation between PL intensity and the surface roughness and Fig. 7 shows the correlation between PL intensity and grain size of the $Gd_{1.82}Eu_{0.10}Li_{0.08}O_3$ films prepared under different reactive atmospheres. It is found from the figure that PL brightness, rms roughness and grain size are highest for the films deposited under oxygen reactive atmosphere. The enhanced PL intensity of the films deposited under oxygen ambient atmosphere may be due to the increase in crystalline size, which reduces the grain boundary density, which may act as a source of dissipation, adsorbing and or scattering light generated inside the film that resulted in lower PL brightness. In addition to that the increased surface roughness of the films may reduce the loss of emitted light due to internal reflections within the film. A simple criteria for the films with enhanced luminescence is that the rougher the surface and less monoclinic phase, the higher the luminescence [11].

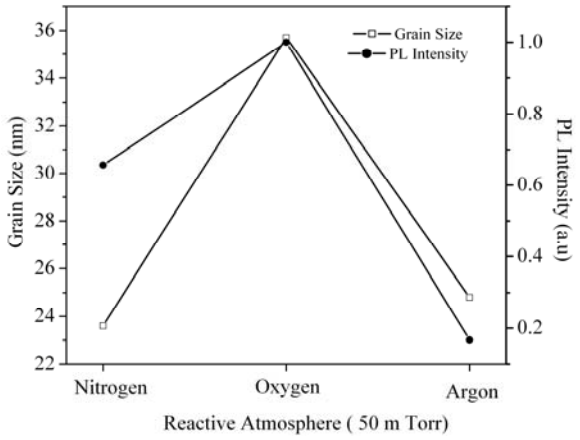

Fig. 7. Plots of PL intensity and grain size of $Gd_{1.82}Eu_{0.10}Li_{0.08}O_3$ films prepared under different reactive atmospheres.

4. Conclusions

High quality $Gd_{1.82}Eu_{0.10}Li_{0.08}O_3$ thin films have been deposited on quartz substrate under oxygen, nitrogen and argon reactive atmospheres using pulsed laser deposition technique. The crystalline phase, surface morphology and surface roughness were found to be very sensitive to the ambient gas, which was used during deposition. The highest emission intensity was observed for the films grown under oxygen reactive atmosphere, whose brightness was 1.52 and 5.97 times higher than that of the films grown under nitrogen and argon ambient atmospheres. The enhanced PL brightness of the films deposited under oxygen reactive atmosphere, suggests that higher the crystalline size, more rougher the surface and less monoclinic phase leading to a strong PL emission at 612 nm. The films prepared under nitrogen ambient atmosphere, the intensity ratio of the 612 nm peak to that of 624 nm peak was found to be higher than that of films deposited under oxygen and argon atmospheres. The increased spectral purity of these films may result from the fact that a smaller fraction of Eu^{3+} ions sit in the surface layers as compared to other samples.

References

[1] T. Hirari, T. Hirano, I. Komasawa, J. Colloid Interface Sci. **253,** 62 (2002).
[2] C.H.Kim, E.II.Kwon, C.H.Cicillini, J.Alloys and Compounds **311,** 33 (2000).
[3] J. Y. Choe, D. Ravichandran, S. M. Blomquist, D. C. Morton, K.W.Kirchner, M.H.Ervin, U.Lee, Appl.Phys.Lett. **78,** 3800 (2001).
[4] Bazzi R, J.Colloid Interface Sci. **273,** 191 (2004).
[5] R. W. Siegel, E. Hu, D. M. Cox, H. Goronkin, L. Jelinski, C. C. Koch, M. C. Roco, D. T. Shaw, Nanostructure Science and Technology, International Technology Research Institute, 1998.
[6] R. P. Andres, Mater.Res **4,** 704 (1989).
[7] K. C. Mishra, J. K. Berkowitz, K. H. Johnson, P. C. Schmidit, Phys. Rev.B **45,** 10902(1992).
[8] R. C. Ropp, The chemistry of Artificial Lighting devices: Lamps, Phosphors and Cathode Ray Tubes, Elsevier, New York 1993.
[9] S. Itoh, T. Kimizuka, T. Tonegawa, J. Electrochem. Soc. **136,** 1819(1989).
[10] H.C. Swart, J.S.Sebastian, T.A.Trottier, S.L. Jones, P.H. Holloway, T.Tonegawa, J. Vac. Sci. Tech. A **14,** 1697(1996).
[11] S.Y.Seo, S. Lee, H.D.Park, N.Shin, K.S.Sohn, J.Appl.Phys. **92**, 5248 (2002).
[12] J.C. Park, H.K. Moon, D.K.Kim, S.H.Byeon, B.C.Kim, K.S. Suh, Appl.Phys.Lett. **77**, 2162 (2000).
[13] S.S. Yi, J.S. Bae, B.K.Moon, J.H.Jeong, J.C.Park, I.W. Kim, Appl.Phys.Lett. **81**, 3344 (2002).
[14] S.S. Yi, J.S. Bae, K.S.Shim,J.H.Jeong, J.C.Park, P.H. Holloway, Appl.Phys.Lett. **84,** 353 (2004).
[15] S.S. Yi, J.S. Bae, B.K.Moon, J.H.Jeong, J.H.Kim, Appl.Phys.Lett. **86,** 071921 (2005).
[16] S.L.Issler, C.C. Torardi, J.Alloy.Compd. **229**, 54 (1995).
[17] Liqin Liu, En Ma, Renfu Li, Guokui Liu, Xueyuan Chen, Nanotechnology **18**, 015403 (2007).
[18] Heesun Yang, Hyeokjin Lee, Paul .H. Holloway, Nanotechnology **16**, 2794 (2005).
[19] Kuo-Min Lin, Yuan-Yao Li, Nanotechnology **17**, 4048 (2006).
[20] Kuo-Min Lin, Chih-Cheng Lin, Yuan-Yao Li, Nanotechnology **17,** 1745 (2006).
[21] Y.C.Kang, I.W.Lenggoro, S.B.Park, K.Okuyama, J.Phys.Chem.Solids. **60**, 1855 (1999).
[22] G.R. Bai, H.Zhang, C.M.Foster, Thin Solid Films **321**, 115(1998).
[23] H.C. Le, R.W.Dreyfus, W.Marine, M.Sentis, I.A.Movtchan, Appl. Surf. Sci. **164,** (1996).
[24] E.E. Fullerton, I.K. Schuller, Y. Bruynseraede, MRS Bull. **17**, 33 (1992).
[25] T.J. Vink, M.A.J. Somers, J.L.C. Daams, A.G. Dirks,J. Appl. Phys. **70**, 4301 (1991).
[26] S.Zhang and R.Xiao, J.appl.Phys.**83**,3842 (1998).
[27] S.L.Jones, D.Kumar, R.K.Singh and P.H.Holloway, Appl.Phys.Lett. **71**, 404(1997).
[28] B. D. Cullitty: Elements of X-ray diffraction, Addison–Wesley, London 1978.
[29] A. V. Bulgakov and N.M.Bulgokava, J. Phys. D: Appl. Phys. **31**, 693 (1998).
[30] Li-Chyng Chen in Pulsed Laser Deposition of Thin Films, Edited by D. B. Chrisey G. K. Hubler (Wiley, New York, 1994) Chap. 6, P.186
[31] Y.Nakanishi, H.Wada, H.Kominami, M.Kottaisamy, T.Aoki, Y.Hatanaka, J.Electrochem.Soc. **146**, 4320 (1999).

[32] K. G. Cho, D. Kumar, S. L. Jones, D. G. Lee, P. H. Holloway, R. K. Singh, J. Electrochem. Soc. **145**, 3456 (1998).
[33] G.Blasse, B. C. Grabmaier, Luminescent Materials, Springer, Berlin, (1994).
[34] M. Sekita, H. Haneda, Shirasaki, T. Yanagitani, J. Appl. Phys **69**(6), 3709 (1991).
[35] Y. M. Ji, D. Y. Jiang, J. L. Shi, J. Lumin, **122-123**, 984 (2007).
[36] J. W. Wang, H. W. Song, X. G. Kong, H. S. Peng, B. J. Sun, B. J. Chen, J. H. Zhang, W. Xu, J. Appl. Phys **93,** 1482 (2003).

*Corresponding author: gopchandran@yahoo.com